Biosensors and Bioelectronics 26 (2011) 4591–4595

Contents lists available at ScienceDirect

Biosensors and Bioelectronics

journal homepage: www.elsevier.com/locate/bios

Short communication

An autonomous CMOS hysteretic sensor for the detection of desorption-free DNA hybridization

Kang-Ho Lee [a], Suk-Hwan Choi [a], Jeong-Oen Lee [a], Mi-Jin Sohn [b], Jun-Bo Yoon [a], Gyu-Hyeong Cho [a,*]

[a] School of EECS, Korea Advanced Institute of Science and Technology, 335, Gwahakro, Yuseong-gu, Daejeon 305-701, Republic of Korea
[b] Korea Research Institute of Bioscience and Biotechnology, 111, Gwahakro, Yuseong-gu, Daejeon 305-806, Republic of Korea

ARTICLE INFO

Article history:
Received 6 January 2011
Received in revised form 14 April 2011
Accepted 21 April 2011
Available online 28 April 2011

Keywords:
Capacitance
DNA hybridization
Desorption
Impedance
Sensor

ABSTRACT

This paper describes a sensor for label-free, fully electrical detection of DNA hybridization based on capacitive changes in the electrode–electrolyte interface. The sensor measures capacitive changes in real time according to a charging–discharging principle that is limited by the hysteresis window. In addition, a novel autonomous searching technique, which exclusively monitors desorption-free hybridized electrodes among electrode arrays, enhances the performance of the sensor compared with conventional capacitive measurement. The sensor system achieves a detection range of 80 dB. The integrated circuit sensor is fabricated with a 0.35 μm CMOS process. The proposed sensor offers rapid, robust and inexpensive measurement of capacitance with highly integrated detection circuitry. It also facilitates quantitative evaluations of molecular densities on a chip with distinctive impedance variations by monitoring desorption-free hybridized electrodes. Our electrical biosensor has great potential for use with bio analytical tools and point-of-care diagnosis.

1. Introduction

DNA sensors are important in diagnostic tests for genomics studies and in early cancer detection and drug discovery (Moore, 2001). Most DNA hybridization detection techniques require the attachment of target molecules, such as fluorescent, chemiluminescent or redox labels (Boon et al., 2002; Kricka, 1999). However, these techniques are costly, time-consuming, and relatively bulky for portable devices; they also have integration difficulties. Label-free nanomechanical oscillating systems, such as cantilever and QCM type devices, have developed by observing changes in the resonant frequency of the oscillation through mass sensing (Burg et al., 2007; Hong et al., 2009). However these devices have the limitation of spatial distance and measurement environment in vacuum or air. Even if they are label-free, these devices are difficult to integrate with readout circuitry and require costly fabrication technology. Fully electrical detection is a promising approach for label-free devices. Several devices are based on the basic field effect transistor, FET, which incorporates nanowire (Zhang et al., 2008) and carbon nanotube (Martinez et al., 2009). These works are limited by the ionic strength of the transport buffer and the low reproducibility due to complex fabrication. Here, the proposed impedance measurement approach using planar electrodes is fully compatible with the standard complementary metal oxide semiconductor (CMOS) process and benefits from the use of low-cost, rapid and highly integrated DNA sensors. A previous work (Moreno-Hagelsieb et al., 2007) proposed an impedance measurement based on the excitation of the sinusoidal voltage, but it is complex: it involves accurate measurement of the phase shift and amplitude of the signal that responds to the excitation. Some studies were based on the excitation of high and low alternating voltage in a pulse shape to investigate the capacitive property in the electrode–solution interface (Guiducci et al., 2004; Stagni et al., 2007). But, through this approach, the impedance characteristics responding to the fixed operating frequency are difficult to be allowed accurately because the transient edge of the supplied pulses includes the entire spectrum of frequency.

This paper proposes label-free detection technology based on real-time measurement of the capacitance using a hysteretic window control method. The proposed method is compact and can be easily digitized; as a result, it has an efficient interface for external digital devices. In addition, the current excitation in this work enables the controllability of the operating frequency and a low sensitivity of noise.

In impedance spectroscopy, the measured capacitance depends largely on the uniformity and density of the molecular monolayers on the electrode surface. The desorption phenomenon, which involves the release of molecules from an electrode surface, is likely enough to occur in experiments that use an affinity property such as DNA hybridization and to bring many problems.

* Corresponding author. Tel.: +82 42 350 3424; fax: +82 42 350 8024.
E-mail address: ghcho@ee.kaist.ac.kr (G.-H. Cho).

0956-5663/$ – see front matter © 2011 Elsevier B.V. All rights reserved.
doi:10.1016/j.bios.2011.04.033

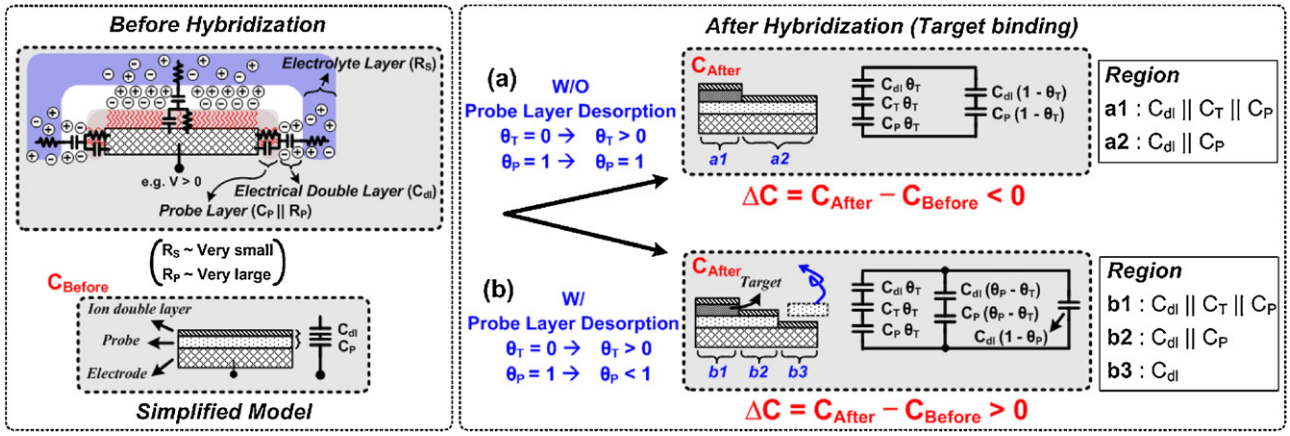

Fig. 1. Illustrations of the capacitance-based modeling before and after the hybridization. This modeling includes both the desorption of the probe DNA layer and the deposition of the target DNA layer; The subscripts *P* and *T* represent the probe and target DNA, respectively. C_P is the specific electrical capacitance of the probe layer, θ_P is its fractional coverage, C_T is the specific electrical capacitance of the target DNA layer, θ_T is its fractional coverage and C_{dl} is the electrical double layer capacitance of the interface with the solution. (a) The binding of target DNA without the desorption of probe DNA results in a decrease of the effective capacitance. (b) The probe-layer desorption results in an increase of the effective capacitance.

Desorption is caused by a careless physical scratch, the competing process with a complementary target and thermal energy on the surface of the probe-functionalized electrode (Moses et al., 2004; Herne and Tarlov, 1997). The adsorptive contacts of probe DNA may be displaced by the stronger bond of a blocking agent, 6-mercapto-1-hexanol, and the electrostatic repulsion between probe strands (Steel et al., 2000). This desorption removes the chance of hybridization with target molecules and consequently degrades the sensitivity of the sensor. In addition, the unstable capacitive properties induced by the dissociation of thiol-modified probes cause a large standard deviation and poor reproducibility of the measured signal, thereby limiting the performance of the sensor. To solve these problems, some research groups have tried to stabilize the probe layer on the surface of the electrode (Riepl et al., 1999) but the stabilizing process requires additional materials and biological treatments. This paper proposes a novel technology that exclusively searches for well-hybridized desorption-free electrodes among electrode arrays. The sensor's ability to exclude electrodes with unstable capacitive property enhances its sensitivity. This method is also available for application in monolayer studies and surface chemistry fields (Satjapipat et al., 2001).

The sensor was fabricated with a commercial CMOS process using detection method that improves conventional biosensors (Berggren, 1999) in new ways, particularly through a hysteretic window control method and an autonomous searching technique. This approach can be used to mass produce the electrical DNA sensor at low cost.

Influenza is a highly contagious respiratory infection that results in high morbidity and mortality (Werner and Harder, 2006). High pathogenic avian influenza (AI), especially H5 subtypes, which causes disease in both human and poultry, has presented a continuous threat throughout Asia, Europe, and Africa since 2003 (Magalhaes et al., 2010; Deregt et al., 2006). Thus rapid, robust and inexpensive detection of influenza is crucial for disease management, rapid intervention, and a possible reduction of an influenza pandemic. The proposed sensor was demonstrated to achieve specific detection of H5N1 DNA of avian influenza. The recent research to synthesize nanoparticles for detecting influenza virus has been demonstrated (Wu et al., 2011; Ting et al., 2009). Although our detection method is less sensitive than state-of-the-art label-dependent methods (Ting et al., 2009) that have sensitivities in the femtomolar range, we are trying to propose that the electrical impedance sensing device can function as label-free transducer for a specific and inexpensive DNA biosensor.

2. Methods

2.1. A study of electrical circuit models

The electrical circuit models are investigated since the sensor is based on the electrical detection of capacitive changes in the electrode–electrolyte interface. Fig. 1 shows a description of capacitance-based modeling that includes both the desorption of probe DNA layer and the deposition of target DNA layer. In Fig. 1(left), the electrode–solution interface including the probe DNA can be modeled with an equivalent circuit composed of resistance (R_P) and capacitance (C_P) in parallel, an electrical double ion capacitive layer (C_{dl}) and solution resistance (R_S) in series. R_P is relative to the property of the insulating layer, which has little effect on the impedance of the electrode–solution interface due to its large value, so R_P can be considered negligible for a dense layer. C_P is generated by the interface between the metal electrode and a quasi-electrode in the electrolyte. This quasi-electrode is the layer of counter-ions attracted to the polarized metal surface with the distance corresponding to the size of the probe DNA (Lee et al., 2010). The R_S depends on the electrolyte solution characteristic, which has such a small value as to be negligible. Therefore, the effective impedance associated with the electrode–solution interface is considered to be composed of the C_P and C_{dl} in series before hybridization, while the C_P, C_T and C_{dl} are in series after binding of the probes and the targets. Here, the electrical capacitance of the probe or target DNA (C_P and C_T, respectively) is about 100 times less than a C_{dl} value (Mirsky et al., 1997); hence, the contribution of the C_{dl} series is negligible. Fig. 1(a) and (b) investigates the changes of impedance without and with the desorption of the probe layer during DNA hybridization.

Fig. 1(a) depicts a case where the probe DNA layer remains the same without any desorption during hybridization. When complementary target DNA strands bind uniformly and densely with the surface probes, there is an increase in the distance between the electrical charge inside the electrode and the ions layer in the electrolyte. Thus, the effective capacitance is consequently decreased (Berggren, 1999; Guiducci et al., 2004). The variation in the effective capacitance can be expressed as follows:

$$\Delta C = C_P \left\{ \theta_T \left(\frac{C_T}{C_P + C_T} - 1 \right) + 1 \right\} < 0 \quad (1)$$

where C_P is the specific electrical capacitance of the probe layer, C_T is the specific electrical capacitance of the target DNA layer and

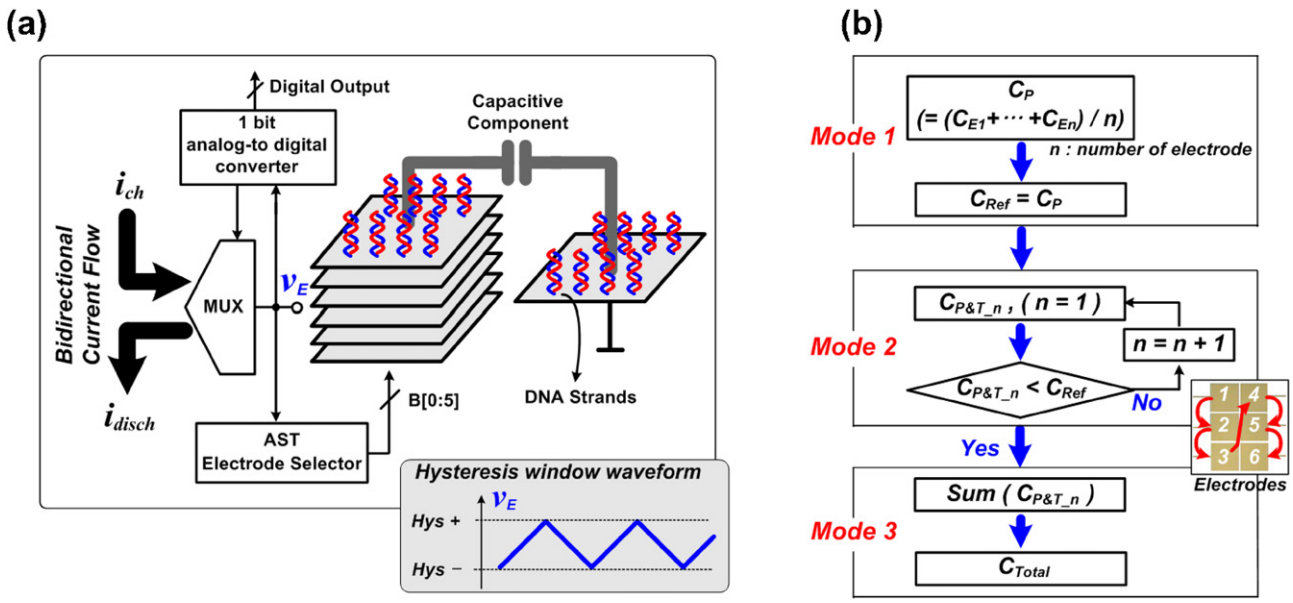

Fig. 2. (a) The capacitive detection method with the hysteresis window control. The voltage of the impedance is increased or decreased by the excitation of the bidirectional current flow. (b) Algorithm of the electrode selector for the AST; $C_{P\&T}$ is the capacitance of the electrode hybridized with the probe and target DNA. The capacitance values of C_P and $C_{P\&T}$ are compared sequentially to search for desorption-free electrodes among electrode arrays.

θ_T is its fractional coverage. From (1) without the desorption of the probe DNA, we can deduce that the binding of the target DNA on an electrode functionalized with probe strands increases the dielectric thickness at the binding sites, resulting in a decrease of the effective capacitance. On the other hand, in Fig. 1(b), the desorption of the probe DNA layer directly exposes the surface of the electrode at the interface with the solution, resulting in an essential increase of impedance by the C_{dl}-induced capacitance. In this case, the change in effective capacitance before and after the hybridization of the probe and target DNA is expressed by

$$\Delta C = C_P \left\{ \theta_T \frac{C_T}{C_T + C_P} + (\theta_P - \theta_T) - 1 \right\} + C_{dl}(1 - \theta_P) > 0 \qquad (2)$$

where θ_P is the fractional coverage of the probe DNA layer. Equation (2) shows that the targets bound on the surface of electrodes with the probe-layer desorption increase the effective capacitance due to the C_{dl}. This desorption of the probe layer is depicted by simplified illustration in 'b3 region' of Fig. 1(b).

Therefore we can identify the electrodes with the probe desorption through the electrical modeling in this study. These electrical models suggest that the sensor can be more sensitive if it exclusively monitors electrodes that showed a decreased change of capacitance, as in Fig. 1(a), and then includes them in the total impedance. The proposed electrical-models are analyzed in detail in the supplementary material (Fig. S-1).

2.2. Design of a hysteretic CMOS sensor system (hysteretic window control method (HWC))

The previous work based on the excitation of high and low alternating voltage in a pulse shape does not identify accurate impedance characteristics responding to the operating frequency and has a high sensitivity of noise (Guiducci et al., 2004; Stagni et al., 2007). We proposed the HWC method, which measures the hybridization of DNA strands by monitoring the rate of change of the electrode voltage based on a current charging–discharging principle within the hysteresis window levels. As shown in Fig. 2(a), each electrode is subject to a periodic current excitation, i_{ch} and i_{disch}. The electrode pairs respond to the charging–discharging current while changing their terminal voltage, V_E. The time constant of the transient waveform in the voltage is determined by the impedance components between two electrode plates. The impedance of electrodes is dominated mainly by the capacitive component of the electrodes due to very high parallel resistance, R_P, as in Fig. 1(left) (Mirsky et al., 1997). Thus, the electrode voltage excited by the bidirectional current flow increases or decreases in a near straight line as shown in hysteresis window waveform of Fig. 2(a). The time required for the voltage to reach the hysteresis window levels depends on the effective capacitance value of the electrodes. The V_E is then transformed into a square signal through a 1-bit analog-to-digital converter. If the high parallel resistance is perfectly ignored, the frequency of the square signal is proportional to the rate of change of the voltage and can be expressed as follows:

$$\frac{1}{f} = \frac{2VC}{I} \qquad (3)$$

where f is the frequency of square signals, V is the hysteresis window level, C is the effective capacitance on the electrode and I is the excited current value.

The transformed square signals are counted within predefined periods and then interfaced with external digital devices. The block diagram and the design considerations are explained in detail in the supplementary material (Fig. S-2-1).

2.3. Autonomous desorption-free searching technique (AST)

The proposed AST searches exclusively for well-hybridized desorption-free electrodes among electrode arrays. Fig. 2(b) shows the algorithm of the proposed AST. The readout circuitry includes six readout channels and one reference channel, and each channel is connected to external electrodes. In mode 1, the capacitance of the electrode functionalized with probe DNA only, C_P, is stored and considered as a reference capacitance, C_{Ref}. Then the C_{Ref} is compared sequentially with the corresponding values measured after the hybridization with the target DNA, $C_{P\&T}$, in mode 2. The difference between C_P and $C_{P\&T}$ is determined through an AST electrode selector, which compares the rate of voltage change in each electrode under the same current bias. The output signal of

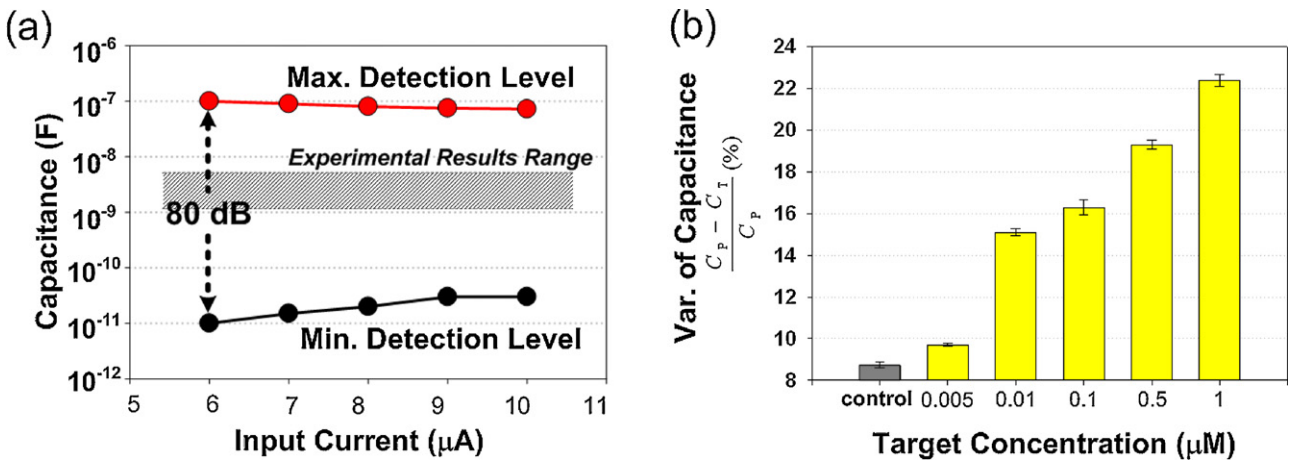

Fig. 3. Measured performance of the designed chip in terms of (a) the detectable impedance range (b) the experimental results for the hybridization of the probe DNA and the target DNA with different concentrations of the targets (5 nM, 10 nM, 100 nM, 500 nM, 1 μM). Control sample includes non-complementary DNA (1 μM).

AST electrode selector is used as an indicator to note whether each electrode is included in the electrode candidates for the total capacitance. The AST electrode selector is explained in detail in the supplementary material (Fig S-2-2). In mode 3, the total capacitance value is obtained by gathering and connecting the selected electrodes. The proposed AST enhances the performance of the sensor by excluding the electrodes with an unstable capacitive property.

2.4. Sensor fabrication and experimental setup

In this paper, the DNA sensor was fabricated with a 0.35 μm CMOS process. Six Au-electrodes immobilized by DNA strands were patterned on the glass by a lift-off process. The active area of the chip was 0.5 mm^2 and that of Au electrodes was 1.5 mm^2 in total. A prototype measurement board included the designed biosensor and electrode arrays separately.

2.5. DNA oligonucleotide and surface preparation

Oligonucleotide sequences derived from an H5N1 avian influenza are CCA AGC AAC AGA CTC AAA (Bioneer Co., Republic of Korea) (Pipper et al., 2007). In this work, we designed the target DNA adding the extra T oligonucleotides of 3-mer to provide a sufficient change of capacitance in the electrode–electrolyte interface (5′-**TTT** CCA AGC AAC AGA CTC AAA-3′) (Stagni et al., 2007). The thiol-functionalized probes, which were modified with a chain of six carbon atoms as a spacer, have a sequence that is complementary to that of the oligonucleotide from the H5N1. The sequences of the non-specific target used as a negative control to verify the hybridization between the probe and complimentary target strands were as follows: 5′-AAC GTA CCT GTC TGT CCC-3′.

Before performing a DNA experiment, the gold electrodes were cleaned thoroughly in a piranha solution (1:3 (v/v) 25% H_2O_2/75% H_2SO_4) for 1 min, rinsed in deionized water, and then dried with nitrogen gas. A layer of 10 μM DNA probes was constructed on each electrode by incubating the surface of the chip in a phosphate buffered saline containing 0.1% Tween (PBST) solution for 6 h at room temperature. After the probe immobilization step, the surface of the chip was immersed in a 10 mM mercapto-hexanol in ethanol for 15 min at room temperature; this process passivates the un-reacted electrode surface and reduces the non-specific binding of the probes and the targets. Target DNA strands were hybridized with probes in 5× SSC buffer containing 0.1% SDS to reduce the electrostatic repulsion between probe strands. All impedance measurements were done in 1× PBS at room temperature. Each concentration of the target DNA was measured at least three times.

3. Results and discussion

The proposed hysteretic biosensor results in the output signal of a square shape, which is within the hysteresis window, and the frequency of this square signal is in inversely proportion to the measured capacitance.

3.1. The performance of the designed CMOS sensor

Fig. 3(a) shows the target range that our biosensor system can measure. The sensor achieves a detection range of 80 dB for the capacitance as well as sensitivity of approximately 10^{-11} F. The performance of this biosensor was investigated with various input currents using off-chip discrete components. The performance is limited by the nonlinearity, the mismatch and the offset of the designed components, such as comparator, current source and, etc., in the platform. However, a range of 80 dB is wide enough to deal with the realistic results in our experiments. These detection and sensitivity are favorably comparable with other biosensor platforms (Moreno-Hagelsieb et al., 2007; Stagni et al., 2006).

3.2. Experimental results

In this paper, three conditions required to verify the proposed biosensor system are as follows: (1) an electrode immobilized with probe DNA, (2) an electrode hybridized specifically with complementary DNA strands, (3) an electrode bound with non-complementary DNA strands. Moreover, measurements with and without AST were compared after injection of the target DNA with the different number of the desorbed electrodes (Fig. S-4 in the supplementary material).

Fig. 3(b) shows the experimental results for the hybridization of the probe DNA and the target DNA for five different concentrations of the targets. The increase in distance of the ion-layer from the polarized electrode resulted from hybridization between probe DNA and complementary DNA can greatly affect the effective capacitance in the electrode–electrolyte interface. In Fig. 3(b), specific DNA binding with complementary samples leads to more significant changes than that of non-complementary samples. The detection limit of the sensor used in this study was 5 nM and capacitance was changed linearly with the target concentration. The capacitance change at specific binding became closer to that

of nonspecific binding with non-complementary DNA as the target concentration decreased because it is difficult for an additional layer of target DNA strands to form densely at a low concentration. The maximum relative variation of capacitance was 22.38% with 1 μM complementary target DNA, while only 8.73% was observed with non-complementary strands. The sensor can detect the target DNA in concentrations ranging from 5 nM to 1 μM with a detection limit of 5 nM. To demonstrate the specificity of our sensor, we investigated two cases where nonspecific binding of oligonucleotides to the sensor surface can affect sensor response. First we successfully detected large sequence lengths of oligonucleotides within human serum. This experiment was spiked in a H5N1 negative serum including a 96-mer target DNA mimic (Fig. S-5 in the supplementary material). Second, the device can identify a single-base mismatch in 18-mer oligonucleotides (Fig. S-6 in the supplementary material).

These data demonstrate that the proposed biosensor is capable of detecting and quantifying the hybridization of probe and target DNA under the condition of the desorption of a probe layer as well as a stable layer.

4. Conclusion

This paper introduced a biosensor for label-free, fully electrical detection of DNA hybridization; the sensor was fabricated with a standard CMOS process. The proposed impedance measurement used a compact and noise-immune hysteretic window control and an autonomous searching technique for desorption-free electrodes. In contrast with sensors used in other works, our sensor offers rapid, robust and inexpensive measurement of capacitance in real time. It also facilitates quantitative evaluation of molecular densities on a chip with distinctive impedance variations by monitoring desorption-free hybridized electrodes. Our electrical biosensor has great potential for use with bioanalytical tools and point-of-care diagnosis.

Acknowledgments

This work was supported by the National Research Foundation of Korea (NRF) grant funded by the Korea Government (MEST) (No. 2010-0027802). The authors would like to thank S.K. Kim in Samsung Advanced Institute of Technology for supporting the biological experiments.

Appendix A. Supplementary data

Supplementary data associated with this article can be found, in the online version, at doi:10.1016/j.bios.2011.04.033.

References

Berggren, C., 1999. Electroanalysis 3 (11), 156–160.
Boon, E.M., Salas, J.E., Barton, J.K., 2002. Nucleic Acid Research 20, 282–286.
Burg, T.P., Godin, M., Knudsen, S.M., Shen, W., Carlson, G., et al., 2007. Nature 446, 1066–1069.
Deregt, D., Furukawa-Stoffer, T.L., Tokaryk, K.L., Pasick, J., Hughes, K.M., HooperMcGrevy, K., Baxi, S., Baxi, M.K., 2006. Journal of Virological Methods 137, 88–94.
Guiducci, C., Stagni, C., Zuccheri, G., Bogliolo, A., Benini, L., Samori, B., Ricco, B., 2004. Biosensors and Bioelectronics 19 (8), 781–787.
Herne, T.M., Tarlov, M.J., 1997. Journal of American Chemical Society 119, 8916–8920.
Hong, S.R., Choi, S.J., Jeong, H.D., Hong, S., 2009. Biosensors and Bioelectronics 24 (6), 1635–1640.
Kricka, L.J., 1999. Clinical Chemistry 45, 453–458.
Lee, K.H., Lee, J.O., Sohn, M.J., Lee, B., Choi, S.H., Kim, S.K., Yoon, J.B., Cho, G.H., 2010. Biosensors and Bioelectronics 26, 1373–1379.
Magalhaes, R.J.S., Ortiz-Pelaez, A., Thi, K.L.L., Dinh, Q.H., Otte, J., Pfeiffer, D.U., 2010. BMC Veterinary Research 6 (10), 1–10.
Martinez, M.T., Tseng, Y.C., Ormategui, N., Loinaz, I., Eritja, R., Bokor, J., 2009. Nano Letters 9 (2), 530–536.
Mirsky, V.M., Riepl, M., Wolfbeis, O.S., 1997. Biosensors and Bioelectronics 12, 977–989.
Moore, S., 2001. IEEE Spectrum 38, 54–60.
Moreno-Hagelsieb, L., Foultier, B., Laurent, G., Pampin, R., Remacle, J., Raskin, J.-P., Flandre, D., 2007. Biosensors and Bioelectronics 22, 2199–2207.
Moses, S., Brewer, S.H., Lowe, L.B., Lappi, S.E., Gilvey, L.B.G., Sauthier, M., Tenent, R.C., Feldheim, D.L., Franzen, S., 2004. Langmuir 20, 11134–11140.
Pipper, J., Inoue, M., F-P-Ng, L., Neuzil, P., Zhang, Y., Novak, L., 2007. Nature Medicine 13, 1259–1263.
Riepl, M., Mirsky, V.M., Novotny, I., Tvarozek, V., Rehacek, V., Wolfbeis, O.S., 1999. Analytica Chimica Acta 392, 77–84.
Stagni, C., Guiducci, C., Benini, L., Ricco, B., Carrara, S., Samori, B., Paulus, C., Schienle, M., Augustyniak, M., Thewes, R., 2006. IEEE Journal of Solid-State Circuits 41 (12), 2956–2964.
Stagni, C., Guiducci, C., Benini, L., Ricco, B., Carrara, S., Paulus, C., Schienle, M., Thewes, R., 2007. IEEE Sensors Journal 7 (4), 577–585.
Satjapipat, M., Sanedrin, R., Zhou, F., 2001. Langmuir 17, 7637–7644.
Steel, A.B., Levicky, R.L., Herne, T.M., Tarlov, M.J., 2000. Biophysical Journal 79, 975–981.
Ting, B.P., Zhang, J., Gao, Z., Ying, J.Y., 2009. Biosensors and Bioelectronics 25, 282–287.
Werner, O., Harder, T.C., 2006. In: Kamps, B.S., Hoffmann, C., Preiser, W. (Eds.), Influenza Report 2006. Flying Publisher, Paris, pp. 48–86.
Wu, C.S., Oo, M.K.K., Cupps, J.M., Fan, X., 2011. Biosensors and Bioelectronics 26, 3870–3875.
Zhang, G.J., Chua, J.H., Chee, R.E., Agarwal, A., Wong, S.M., Buddharaju, K.D., Balasubramanian, N., 2008. Biosensors and Bioelectronics 23 (11), 1701–1707.